Jpn. J. Cancer Res. 88, 120–128, February 1997

Overexpression of Integrin-associated Protein (CD47) in Rat Kidney Treated with a Renal Carcinogen, Ferric Nitrilotriacetate

Yasuyuki Nishiyama,[1] Tomoyuki Tanaka,[1] Hiroshi Naitoh,[2] Chisato Mori,[2] Manabu Fukumoto,[1] Hiroshi Hiai[1] and Shinya Toyokuni[1,3]

Departments of [1]Pathology and Biology of Diseases and [2]Anatomy and Developmental Biology, Graduate School of Medicine, Kyoto University, Yoshida-Konoe-cho, Sakyo-ku, Kyoto 606

An iron chelate, ferric nitrilotriacetate (Fe-NTA), induces renal proximal tubular necrosis, a consequence of free radical-associated damage, that ultimately leads to a polycystic change of the renal cortex and a high incidence of renal cell carcinoma (RCC) in rodents. The differential display technique was used to search for inducible genes in the kidney of male Wistar rats treated with Fe-NTA and in the induced RCCs. Six fragments were selected that showed specific quantitative changes in mRNA. Two of them exhibited similar patterns in northern blots as well. One fragment showed a high homology (89%) to murine integrin-associated protein (IAP; CD47). We thus cloned rat IAP cDNA including the entire coding region for use in further analysis. Rat IAP cDNA showed a 21-amino-acid deletion that was also observed in human, but not in mouse. Northern blots revealed that IAP was consistently overexpressed in non-tumorous parts of the kidney (2.4-fold increase, $n=9$, $P<0.0001$) as compared with matched controls 1 to 2 years after Fe-NTA treatment. IAP overexpression of more than 2.9-fold was found in 25% (2/8) of RCCs studied, and was limited to cases of a high histological grade and lung metastasis. Unexpectedly, IAP expression was higher in the non-tumorous part of the kidney after Fe-NTA treatment (2.8-fold) than in RCC (1.5-fold) in each case ($n=4$, $P<0.05$). Abundant expression of IAP mRNA in the renal tubular epithelium after Fe-NTA treatment and RCC cells was observed by *in situ* hybridization. The results suggest that IAP overexpression may be associated with Fe-NTA-induced renal cortical tubular damage and regeneration that lead to a polycystic state, and with tumor progression and metastasis of the induced RCCs.

Key words: Ferric nitrilotriacetate — Oxidative stress — Renal cell carcinoma — Differential display — Integrin-associated protein (CD47)

Nitrilotriacetic acid (NTA) is a synthetic aminotricarboxylic acid that efficiently forms water-soluble chelate complexes with several metal cations at neutral pH. NTA has been used as a substitute for polyphosphates in detergents for household and hospital use in the U.S., Canada and Europe.[1] An experimental model of iron overload was developed by the use of ferric nitrilotriacetate (Fe-NTA).[2] Later, repeated i.p. administration of Fe-NTA was reported to induce acute and subacute renal proximal tubular damage and subsequent development of renal cell carcinoma (RCC) in rats and mice at a high incidence (60–92%).[3,4] We have thus far shown that these lesions induced by Fe-NTA are mediated by reactive oxygen species (ROS).[5–8] Little is known, however, about the change in gene expression in response to the oxidative stress mediated by Fe-NTA.

Fe-NTA-induced RCCs resemble their human counterparts with regard to epithelial origin, invasive and metastatic potential, and histological appearance.[9] We have recently reported a low frequency of *ras* and *p53* gene mutations in this renal carcinogenesis model.[9] In human RCCs, the cancer-related genes are still under investigation, although it has been shown that the von Hippel-Lindau gene is involved in 57% of RCCs of the clear cell subtype.[10] In the present study, we undertook to identify unique genes that change their expression during renal proximal tubular damage, regeneration and renal carcinogenesis by the use of a differential display (DD) method.

MATERIALS AND METHODS

Animals Male specific-pathogen-free Wistar rats (Shizuoka Laboratory Animal Center, Shizuoka) were used. Three kinds of studies, a time-course study of the acute phase ($\leq$24 h after single administration: acute study), a subacute study (1 and 6 weeks) and a carcinogenesis study, were started using rats of 130–150 g (6 weeks of age). They were kept in stainless steel cages and given commercial rat chow (Funabashi F-2, Chiba) as well as deionized water (Millipore Japan, Osaka) *ad libitum*.

Fe-NTA treatment procedure Fe-NTA solution was

[3] To whom correspondence and reprint requests should be addressed.

The sequence reported in this paper has been deposited in the GenBank data base (accession no. D87659).

prepared as previously described.[6] Animals of the acute study received i.p. Fe-NTA injection at 15 mg Fe/kg body weight and were killed after 1, 3, 6, 16, and 24 h. Animals of the subacute and carcinogenesis studies received injections according to the following protocol: 5 mg Fe/kg×3 days, 10 mg Fe/kg×3 days (1 week), 1-day break; plus (10 mg Fe/kg×5 days, 2-days break)× 5 weeks (6 weeks), or×11 weeks (carcinogenesis protocol) as previously described.[9] Animals of the NTA group received the NTA portion of the Fe-NTA solution. Animals were killed 24 h after the final administration in subacute studies (1 and 6 weeks). The details of the induced RCCs have been described.[9] Kidneys were stored frozen at −80°C for further experiments.

RNA isolation and differential display Total RNA was isolated from each frozen tissue by means of a modified acid guanidinium phenol chloroform method (Isogen, Nippon Gene, Tokyo). RNA was treated with RNase-free DNase using a Messageclean kit (GenHunter Corp., Brookline, MA). Differential mRNA display was performed using RNA map kits A (GenHunter Corp.) according to the manufacturer's recommendation. Briefly, 0.1 μg of total RNA was transcribed with the anchored primers [$d(T)_{12}$-NG/NC/NA/NT]. Then PCR was done using the corresponding anchored primers and one of the three arbitrary 10-mers (AP-1: 5′-AGCCAGCGAA-3′, AP-2: 5′-GACCGCTTGT-3′ and AP-3: 5′-AGGTGACCGT-3′) in the presence of [^{35}S]dATP (Amersham, Arlington Heights, IL). The PCR samples were loaded on a 6% sequencing gel. The fragments showing specific expression were cut from the dried gel and reamplified using the corresponding primer set.

Cloning and cDNA sequencing of fragments selected by differential display Reamplified cDNAs extracted from sequencing gel were cloned into the PCR II vector using the TA cloning kit (Invitrogen, San Diego, CA). The plasmid DNAs were sequenced according to the manufacturer's procedure using a Sequenase kit (United States Biochemical Co., Cleveland, OH).

Isolation of cDNA of rat IAP Based on the mouse and human cDNA sequences of integrin-associated protein (IAP) and our clone, we PCR-amplified cDNA of rat IAP from the first strand of the cDNA used in DD. The forward primer was 5′-TGATCCAGACACCTGCG-3′, and the reverse was 5′-AGTCCGTCACTTCCCTTCA-3′. The PCR product of 1012 bp was cloned into the PCR II vector using the TA cloning kit and sequenced.

Northern blot analysis Cloned rat IAP cDNA including the entire coding region was digested with *Eco*R I (Takara, Tokyo). Probes were radiolabeled with [α-^{32}P]dCTP (Amersham) using a Megaprime kit (Amersham). Fifteen or 20 μg of total RNA was electrophoresed on 1% formaldehyde agarose gel, transferred onto a nylon membrane and hybridized to rat IAP cDNA. The signal of β-actin probe[11] was used as a control for mRNA expression. Densitometric determination and imaging were carried out by use of a Bioimaging Analyzer System (BAS2000, Fuji, Tokyo).

***In situ* hybridization** To obtain the RNA probe, IAP cDNA fragment (570 bp) (5′-TGCTCCAGACACCTGCG, 3′-CCAGAACAGGAGTATAGCCA) was amplified by PCR and then cloned using a TA cloning kit. Digoxigenin (dig)-labeled RNA probe was transcribed using T7 and SP6 RNA polymerase with a dig-RNA-labeling kit (Boehringer Mannheim, Penzberg, Germany) according to the manufacturer's protocol. Frozen tissues of RCCs and the non-tumorous part of the renal cortex in the carcinogenesis study (Fe-NTA treatment) were cut at 9 μm in a cryostat and processed for *in situ* hybridization.[12] The slides were fixed with 4% paraformaldehyde in 0.05 *M* phosphate-buffered saline (PBS) at room temperature (RT) for 10 min, treated with 10 μg/ml proteinase K for 10 min at 37°C, and then postfixed with 4% paraformaldehyde in 0.05 *M* PBS at RT for 1 min, followed by five further washes: 0.01 *M* PBS at RT for 1 min, 0.2 *N* HCl at RT for 10 min, 0.01 *M* PBS at RT for 1 min, 0.1 *M* triethanolamine with 0.25% acetic anhydride and 0.01 *M* PBS. The slides were prehybridized for at least 10 min at 42°C with hybridization solution containing 50% deionized formamide and 2× saline sodium citrate (SSC). Then they were incubated with hybridization solution (50% formamide, transfer RNA 1 μg/ml, 2×SSC, sperm DNA 1 μg/ml, BSA 1 μg/ml, dextran sulfate 1 μg/ml) (20 μl/slide) containing dig-cRNA (final concentration 0.1–1.0 μg/ml) at 42°C for 16 h. Finally they were washed in 50% formamide and 2×SSC at 50°C for 40 min, in NTE buffer (0.5 *N* NaCl, 10 m*M* Tris-HCl (pH 8.0), 1 m*M* EDTA) at 37°C for 10 min, in NTE buffer containing 20 μg/ml RNase at 37°C for 30 min, in NTE buffer at 37°C for 10 min, in 2×SSC at 42°C for 20 min and twice in 0.2×SSC at 42°C for 20 min. For immunodetection of the signal, a DIG nucleic acid detection kit (Boehringer Mannheim) was used according to the manufacturer's protocol.

Statistics Statistical analyses were performed by using an unpaired *t* test, which was modified for unequal variances when necessary.

RESULTS

Differential display For the DD analysis, we used three arbitrary primers and four anchored primers for a time-course study (control; 1, 3, 6, 16 and 24 h after single Fe-NTA administration; 1 and 6 weeks of repeated Fe-NTA administration) and for analysis of 3 RCCs (No. 3, 14 and 39 of Table I; Fig. 1a). Subsequently, we selected six fragments, the expression of which specifically decreased or increased in accordance with treatment period

Table I. Histology and IAP Expression of Rat Renal Cell Carcinomas Produced by Fe-NTA

No. of case	Histological type[a]				Metastasis and invasion	Expression of IAP	
	Structure	Cell type	Grading	Size (mm)[b]		Tumor	Non-tumorous part
3[c]	solid and tubular	common, granular	G2>G3	30	lung, kidney, liver and peritoneum	0.85	NA[d]
4[c]	solid and papillary	granular and pleomorphic	G2	10	(−)	0.86	NA
14	papillary, tubular and cystic (mixed)	common, granular	G2	20	lung	2.9	NA
17	solid	pleomorphic	G3	50	lung, peritoneum	1.2	2.8
24	solid	pleomorphic	G3	20	lung	4.7	NA
26	cystic and tubular	common, mixed	G1	25	(−)	1.6	3.4
34	solid and tubular	common, granular	G1>G2	35	kidney	1.6	2.7
39	solid	granular and pleomorphic	G2>G3>G1	20	(−)	1.8	1.8

a) Histological classification was according to the modified WHO classification.[30]
b) Size indicates maximal diameter.
c) Cases 3 and 4 are multiple RCCs of a single rat, respectively.
d) NA, not available.

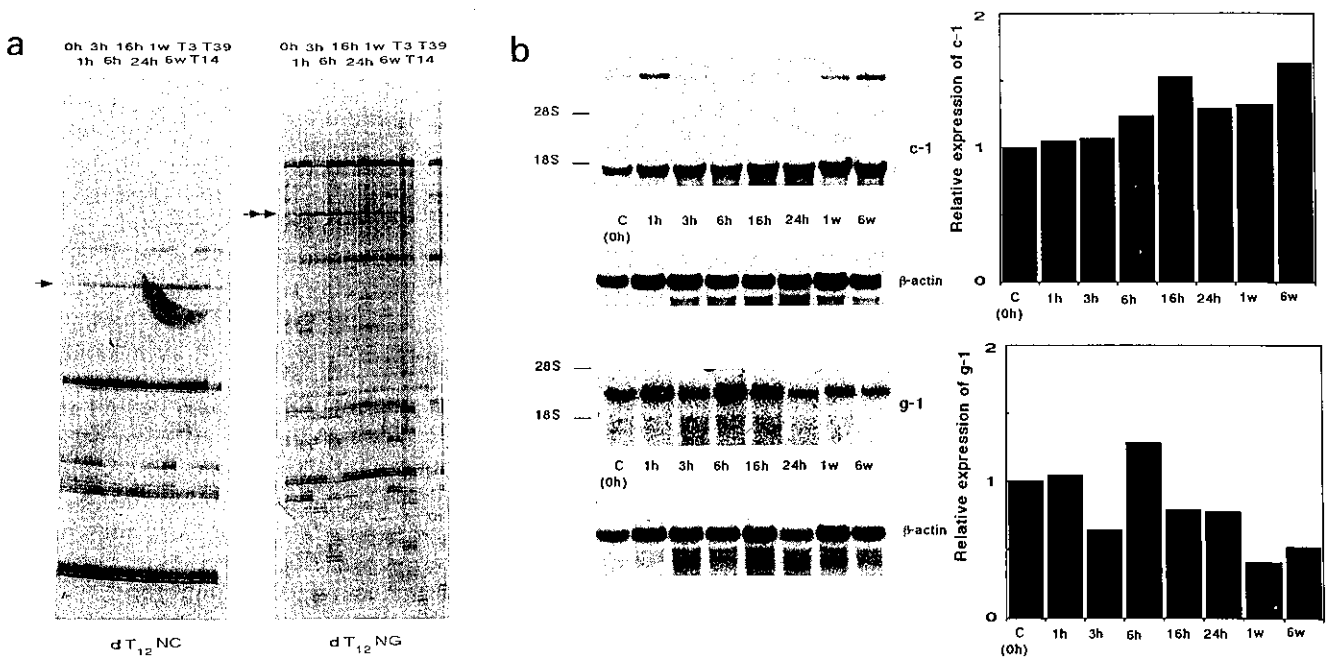

Fig. 1. a, Differentially expressed mRNAs in the kidney at different time points after Fe-NTA administration and in the Fe-NTA-induced RCCs. mRNA was reverse-transcribed with $d(T)_{12}NC$ and an arbitrary 10-mer (AP-1). Lanes 1–11 correspond to: 0, 1, 3, 6, 16 and 24 h (lanes 1–6) after single i.p. administration of 15 mg Fe/kg Fe-NTA; 1 and 6 week (lanes 7 and 8) after repeated i.p. administration of Fe-NTA and three Fe-NTA-induced RCCs (No. 3, 14 and 39 of Table I; lanes 9–11). Arrows indicate differentially expressed candidate cDNAs (single arrow, c-1; double arrow, g-1). b, Northern blot analysis and its histogram at different time points after Fe-NTA administration. Lanes 1–8: 0, 1, 3, 6, 16 and 24 h; 1 and 6 week. Top, c-1; bottom, g-1. See "Materials and Methods" for details.

or carcinogenesis. Two fragments showed the same pattern both by DD and northern blot analyses (Fig. 1b). One fragment (c-1, ~260 bp) showed a continuous increase in expression with time. The other fragment (g-1, ~320 bp) showed a temporary increase in expression at the acute phase and decreased at 1 and 6 weeks. We

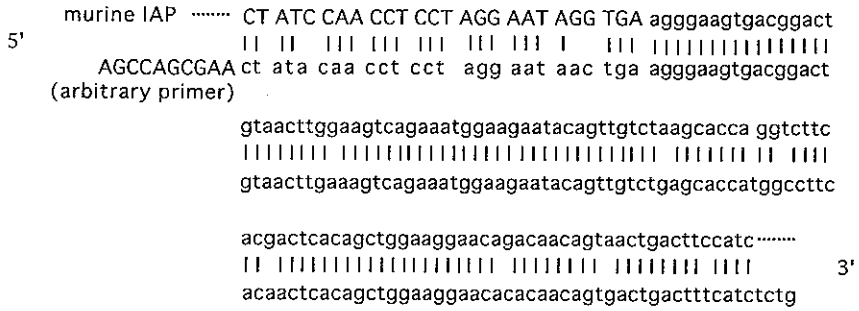

Fig. 2. Nucleotide sequence of c-1. c-1 cDNA fragment sequence and the mouse IAP sequence obtained from GenBank are compared.

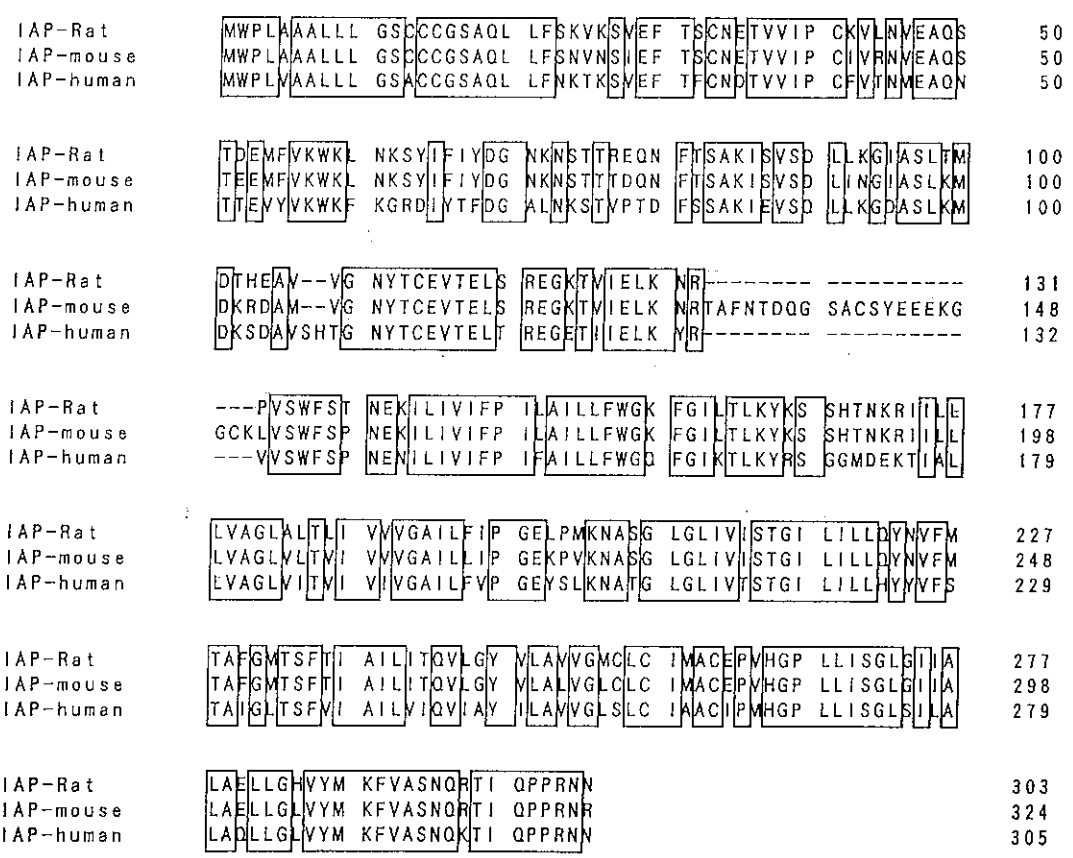

Fig. 3. Amino acid sequences of rat, mouse and human IAP. (–) indicates deletion.

sequenced them and searched for homology by BLAST analyses (Human Genome Center, Institute of Medical Science, University of Tokyo). c-1 was found to have a high homology (89%) (Fig. 2) to mouse integrin-associated protein (IAP; CD47). However, g-1 showed no significant correlation with any published sequence. In the present study, cDNA of rat IAP-homologue was cloned, sequenced and analyzed. Screening of the cDNA library for the g-1 fragment is in progress.

cDNA structure of rat IAP By cDNA cloning of rat IAP, a fragment of 1012 bp was obtained. The amino acid sequence data are shown in Fig. 3. Rat IAP was

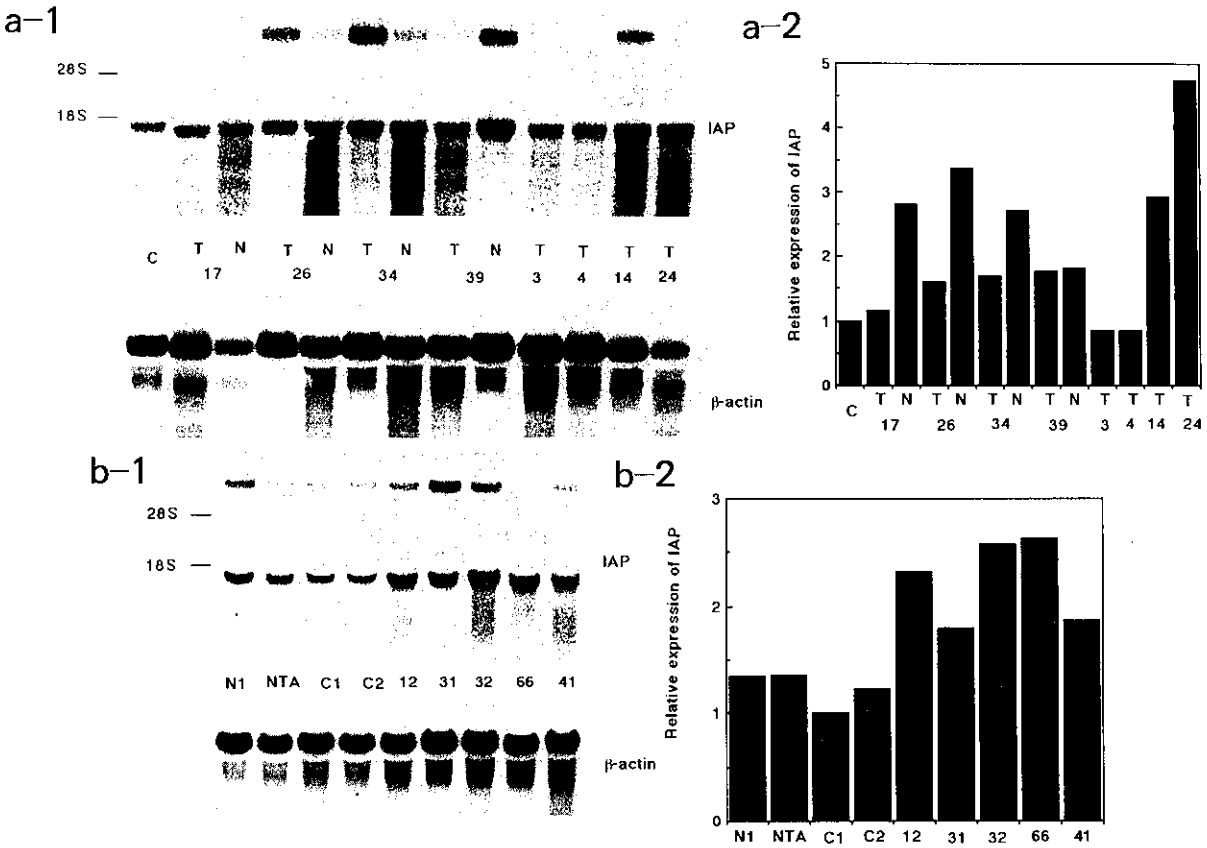

Fig. 4. Northern blot analysis of IAP. Total RNA of each tissue was hybridized with rat IAP cDNA (1012 bp) and β-actin. Radioactivity of bands was measured by densitometry and the results were corrected based on the β-actin hybridization level. Relative mRNA expression levels were calculated as the ratio of sample to control (kidney from normal untreated 5-week-old rat). C, C1, C2, age-matched control; N, non-tumorous part of the kidney; T, tumor (RCC). a-1, RCCs and non-tumorous part of the kidney. Lanes 1–14: C, 17(T), 17(N), 26(T), 26(N), 34(T), 34(N), 39(T), 39(N), 3(T), 4(T), 14(T), 24(T). Case numbers correspond to those of Table I. a-2, Histogram of a-1. b-1, Kidneys of Fe-NTA-treated rats in which RCC was not induced. Lanes 1–9: N1, NTA, C1, C2, 12 [436 days], 31 [554 days], 32 [554 days], 66 [571 days], 41 [597 days]). N1 is a kidney from a 1-year-old normal [689 days] untreated rat. b-2, Histogram of b-1.

more homologous to that of mouse, except for a 21-amino-acid (63 bp) deletion observed in rat and human IAP, but not in mouse IAP.

Northern blot analysis of IAP Northern blot analyses were done on the following samples with our rat IAP cDNA probe in addition to chronological kidney samples after Fe-NTA treatment (Fig. 1b); 1) Fe-NTA-induced RCCs and adjacent non-tumorous parts of the kidney (Fig. 4a), 2) kidneys of Fe-NTA-treated rats in which RCC was not induced (Fig. 4b). In all northern blot analyses two bands (1.4-kilobase and 6-kilobase) were observed, as described by Campbell *et al.*[13]

IAP expression was increased in all the non-tumorous kidney samples after Fe-NTA treatment in the carcinogenesis study, whether RCC was observed or not (2.4-fold on average; $n=9$, $P<0.0001$). There was no statistically significant difference in the level of IAP overexpression in the non-tumorous kidneys whether RCC was induced or not. IAP expression was also increased in 2 out of 8 RCC cases (2.9- and 4.7-fold; Table I). These 2 cases exhibited a high-grade histology (Fig. 5b) and lung metastasis. Furthermore, when each RCC was compared with the adjacent non-tumorous part of the kidney, IAP expression was higher in the non-tumorous part of the kidney (2.8-fold) than in the RCC (1.5-fold) ($n=4$, $P<0.05$; Table I).

Histology Histology of all the specimens used in northern blot analysis was examined. Degeneration of renal proximal tubules began 3 h after single Fe-NTA administration and necrosis became prominent at 16 to 24 h. After 1 or 6 weeks of repeated Fe-NTA treatment, little necrosis was observed, but regenerative proximal tubules

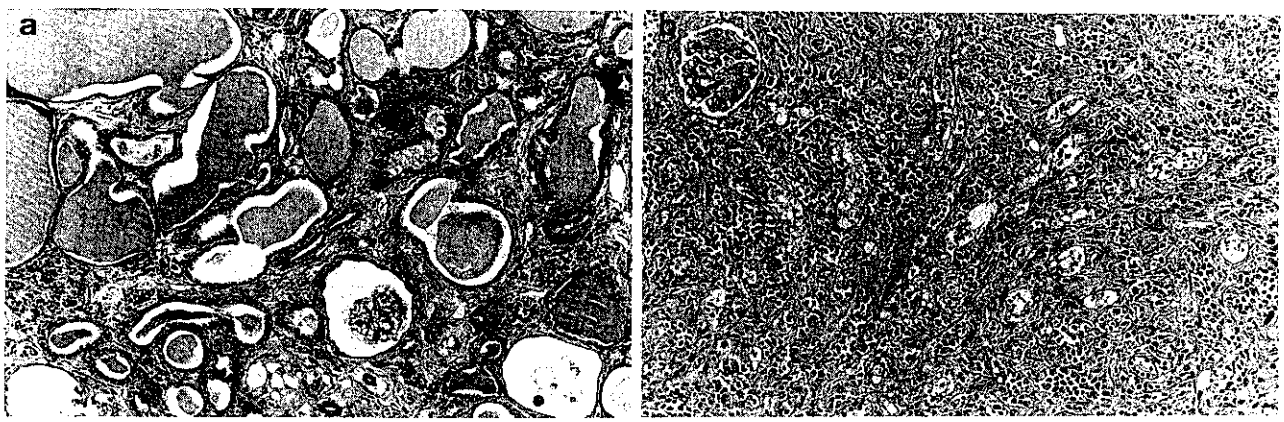

Fig. 5. a, Histology of renal cortex 1 year after treatment with Fe-NTA (No. 66 of Fig. 4, b-1 and b-2). Dilatation of renal proximal tubules (polycystic change) that contain some regenerative atypical cells. Fibrosis, infiltration of inflammatory cells and capillary proliferation in the interstitium are also seen. b, Histology of renal cell carcinoma (No. 24 of Fig. 4, a-1, a-2 and Table I). Proliferation of atypical cells with solid nest formation is seen. (Hematoxylin and eosin, ×85).

containing atypical karyomegalic cells were seen. One to 2 years after Fe-NTA treatment for 12 weeks, renal cortical tubules were dilated and epithelial cells became more flattened and showed a polycystic appearance. Atypical or dysplastic cells were frequently observed in the proximal tubules. In the interstitium, fibrosis with proliferation of fibroblasts and capillary vessels, and infiltration of lymphoid cells were also seen (Fig. 5a). Kidneys of NTA-treated animals showed no apparent difference from those of untreated control animals (data not shown). Table I summarizes the pathological data of RCCs. Fig. 5b shows the histology of an RCC that showed a high IAP expression with lung metastasis.

***In situ* hybridization** *In situ* hybridization study showed an abundant expression of IAP mRNA in the renal tubular epithelium 1 year after treatment with Fe-NTA and RCC cells compared with renal tubular epithelium after 1-week treatment with Fe-NTA (Fig. 6, a, b and c).

DISCUSSION

IAP is a 50-kD membrane protein copurified with the integrin $\alpha_V\beta_3$ from placenta.[14, 15] Functionally, IAP has a role in the activation of leukocytes associated with leukocyte response integrin. It has a single extracellular IgV-like domain and multiple membrane-spanning segments.[15] Recently, it was found that IAP is physically and functionally associated with the integrin $\alpha_V\beta_3$ vitronectin receptor and is involved in the increase in intracellular calcium concentration, which occurs upon cell adhesion to extracellular matrix.[15, 16]

IAP is probably the same protein as CD47 glycoprotein and OA3, originally reported as an ovarian tumor marker.[13, 17] IAP is a broadly distributed protein present in all hematopoietic cells, epithelial cells, endothelial cells, fibroblasts, and tumor cell lines.[14, 17–19] Therefore, it is thought that IAP has a rather general function or an association with other integrins such as integrin $\alpha_V\beta_3$. In our northern blot analyses, IAP was expressed in all the organs examined (heart, lung, liver, spleen, kidney, breast, intestine and testis: data not shown).

We have cloned rat IAP cDNA including the entire coding region. The sequence of rat IAP cDNA has not been reported previously. Rat IAP is more homologous in amino acid sequence to mouse IAP (85%) than to human IAP (70%). However, the 63 bp deletion found in the extracellular domain of rat IAP was observed in human, but not in mouse. Rat and mouse are evolutionarily close, but this deletion appears to have occurred during their brief divergence and has remained in the human genome.

In our study, overexpression of IAP in non-tumorous parts of the kidney was prominent in the chronic phase after 1 year and high IAP expression was seen in some of the induced RCCs (Fig. 4, a and b). Histologically, there were distinct morphological changes in the chronic phase. Cyst formation, regenerated tubular epithelium with cellular atypia, growth of capillaries in the interstitium, infiltration of inflammatory cells and fibrosis were observed (Fig. 5a). By *in situ* hybridization more abundant expression of IAP mRNA in renal tubular epithelium than in glomeruli and interstitium was shown (Fig. 6b). These data confirm that there is an overexpression of IAP mRNA in the renal tubular epithelium. Therefore, renal cortex including renal tubular epithelium appears to be in a state of abnormal cell-cell or

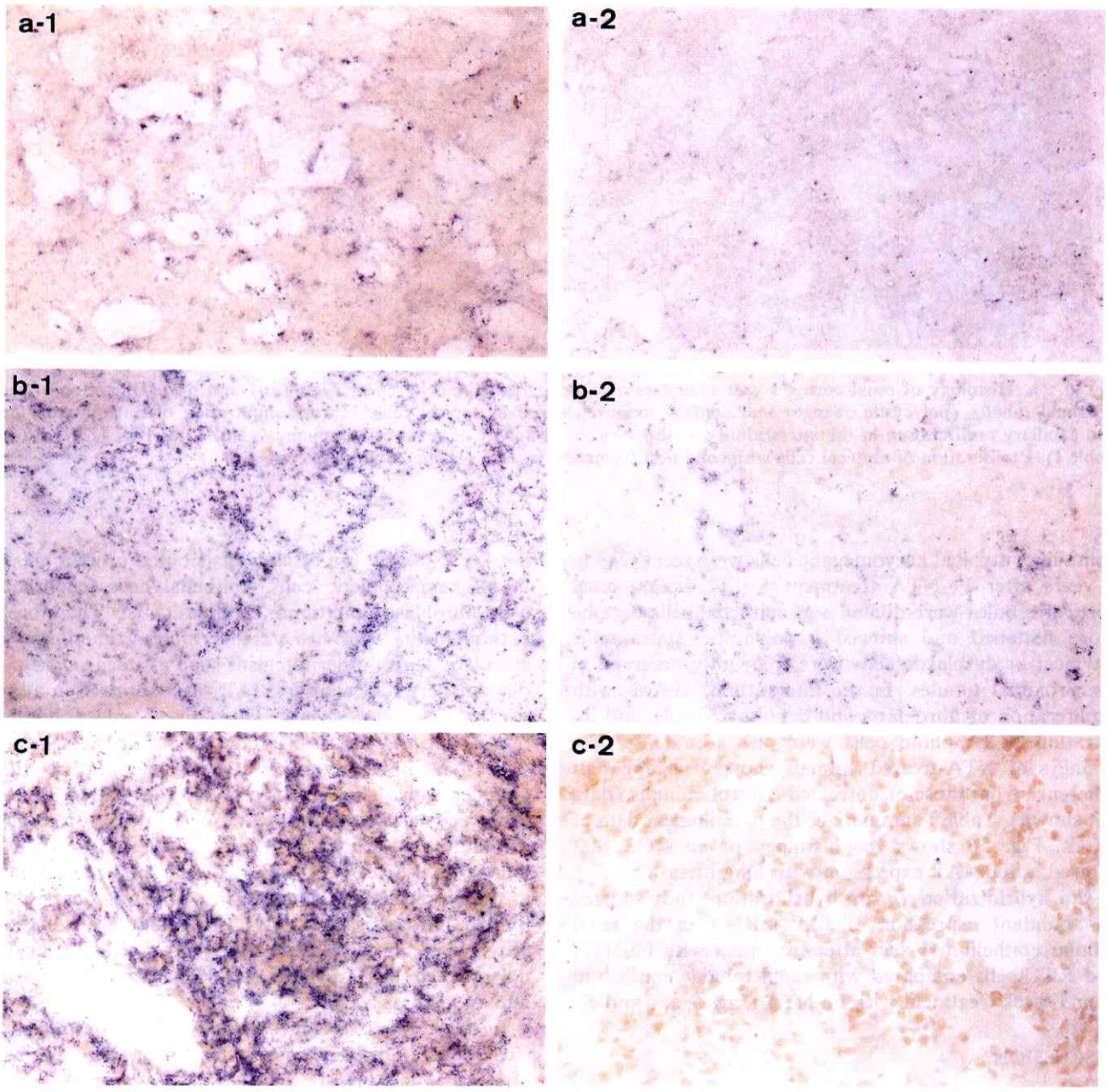

Fig. 6. Expression of IAP mRNA by *in situ* hybridization using digoxigenin-labeled mRNA. a, Renal tubular epithelium 1 week after treatment with Fe-NTA. b, Renal tubular epithelium 1 year after treatment with Fe-NTA. c, Renal cell carcinoma. Note abundant expression of IAP in the renal tubular epithelium 1 year after treatment with Fe-NTA and in the renal cell carcinoma cells compared with renal tubular epithelium after 1-week treatment with Fe-NTA. -1, anti-sense; -2, sense. ×340.

cell-matrix signal transduction, especially regarding Ca^{2+} influx.[16, 20] In a recent report, PKD2 was identified as a candidate gene for polycystic kidney disease.[21] PKD2 protein has an amino acid sequence similarity with the family of voltage-activated calcium channels. It is possible that abnormal Ca^{2+} transport associated with IAP overexpression may accelerate renal polycystic changes. On the other hand, it is known that acquired cystic kidney disease in patients receiving long-term dialysis is a risk factor for RCCs.[22, 23]

Overexpression of IAP was seen in some of the RCC cases by northern blotting. *In situ* hybridization study showed that RCCs themselves overexpressed IAP (Fig. 6c). In a recent study, overexpression of integrin $\alpha_V\beta_3$ on melanoma cell line was suggested to be a key player in cell invasion.[24] On the other hand, overexpression of IAP has been reported on another melanoma cell line.[20] Of note was the fact that RCCs with high IAP expression metastasized to the lung, though the opposite was not true (Table I). It appears that high expression of IAP corresponds to a state of loose connection of epithelial cells, such as a renal polycystic state or high-grade RCC. As IAP is associated with integrin $\alpha_V\beta_3$,[15] these data suggest that IAP has a role in tumor invasion and metastasis.

The DD technique is a powerful and simple method to detect altered gene expression.[25] However, there are sometimes false-positives, and many modified methods have been proposed.[26,27] We applied the DD technique using an RNA map kit to detect chronological changes in the kidney treated with Fe-NTA. We used a variety of samples as a set from the acute study, chronic study and the induced RCCs. We carefully selected fragments that consistently showed specific quantitative changes to minimize false-positives. Using three arbitrary primers, the IAP gene was identified as an Fe-NTA-inducible gene, and expression of IAP mRNA at regenerated tubular epithelium and RCCs was demonstrated by *in situ* hybridization. Little is known so far about the *in vivo* molecular events resulting from the exposure to ROS mediated by transition metals. As early-response genes to oxidative stress by H_2O_2, *myc, jun* and *fos* genes have been found in *in vitro* experiments.[28,29] Our system may be useful to uncover genes concerned with cellular damage by ROS mediated by transition metals.

ACKNOWLEDGMENTS

This work was supported in part by a Grant-in-Aid from the Japanese Ministry of Education, Science, Sports and Culture, and by a grant from the Sagawa Foundation for Promotion of Cancer Research. We thank Dr. James E. Strickland (NCI, NIH, Bethesda, MD) for a critical reading of the manuscript, and Dr. Masashi Kawaichi (Nara Institute of Science and Technology, Nara, Japan) for valuable discussions.

(Received August 14, 1996/Accepted November 19, 1996)

REFERENCES

1) Anderson, R. L., Bishop, W. E. and Campbell, R. L. A review of the environmental and mammalian toxicology of nitrilotriacetic acid. *Crit. Rev. Toxicol.*, **15,** 1–102 (1985).
2) Awai, M., Narasaki, M., Yamanoi, Y. and Seno, S. Induction of diabetes in animals by parenteral administration of ferric nitrilotriacetate: a model of experimental hemochromatosis. *Am. J. Pathol.*, **95,** 663–673 (1979).
3) Ebina, Y., Okada, S., Hamazaki, S., Ogino, F., Li, J.-L. and Midorikawa, O. Nephrotoxicity and renal cell carcinoma after use of iron- and aluminum-nitrilotriacetate complexes in rats. *J. Natl. Cancer Inst.*, **76,** 107–113 (1986).
4) Li, J.-L., Okada, S., Hamazaki, S., Ebina, Y. and Midorikawa, O. Subacute nephrotoxicity and induction of renal cell carcinoma in mice treated with ferric nitrilotriacetate. *Cancer Res.*, **47,** 1867–1869 (1987).
5) Toyokuni, S., Okada, S., Hamazaki, S., Minamiyama, Y., Yamada, Y., Liang, P., Fukunaga, Y. and Midorikawa, O. Combined histochemical and biochemical analysis of sex hormone dependence of ferric nitrilotriacetate-induced renal lipid peroxidation in ddY mice. *Cancer Res.*, **50,** 5574–5580 (1990).
6) Toyokuni, S., Uchida, K., Okamoto, K., Hattori-Nakakuki, Y., Hiai, H. and Stadtman, E. R. Formation of 4-hydroxy-2-nonenal-modified proteins in the renal proximal tubules of rats treated with a renal carcinogen, ferric nitrilotriacetate. *Proc. Natl. Acad. Sci. USA*, **91,** 2616–2620 (1994).
7) Toyokuni, S., Mori, T. and Dizdaroglu, M. DNA base modifications in renal chromatin of Wistar rats treated with a renal carcinogen, ferric nitrilotriacetate. *Int. J. Cancer*, **58,** 291–297 (1994).
8) Uchida, K., Fukuda, A., Kawakishi, S., Hiai, H. and Toyokuni, S. A renal carcinogen ferric nitrilotriacetate mediates a temporary accumulation of aldehyde-modified proteins within cytosolic compartment of rat kidney. *Arch. Biophys. Biochem.*, **317,** 405–411 (1995).
9) Nishiyama, Y., Suwa, H., Okamoto, K., Fukumoto, M., Hiai, H. and Toyokuni, S. Low incidence of point mutations in H-, K- and N-*ras* oncogenes and *p53* tumor suppressor gene in renal cell carcinoma and peritoneal mesothelioma of Wistar rats induced by ferric nitrilotriacetate. *Jpn. J. Cancer Res.*, **86,** 1150–1158 (1995).
10) Gnarra, J. R., Tory, K., Weng, Y., Schmit, L., Wei, M. H., Li, H., Latif, F., Liu, S., Chen, F., Duh, E. M., Lubensky, I., Duan, D. R., Florence, C., Pozzatti, R., Walther, M. M., Bander, N. H., Grossman, H. B., Brauch, H., Pomer, S., Brooks, J. D., Isaacs, W. B., Lerman, M. I., Zbar, B. and Linehan, W. M. Mutations of the VHL tumor suppressor gene in renal carcinoma. *Nat. Genet.*, **7,** 85–90 (1994).
11) Yasuda, K., Yamada, Y., Inagaki, N., Yano, H., Okamoto, Y., Tetsuji, K., Fukumoto, H., Imura, H., Seino, S. and Seino, Y. Expression of GLU1 and GLU2 glucose transporter isoforms in rat islets of Langerhans and their regulation by glucose. *Diabetes,* **41,** 76–80 (1992).

12) Xu, X.-C., Clifford, J. L., Hong, W. K. and Lotan, R. Detection of nuclear acid receptor mRNA in histological tissue sections using nonradioactive *in situ* hybridization histochemistry. *Diagn. Mol. Pathol.*, **3**, 122–131 (1994).
13) Campbell, I. G., Freemont, P. S., Foulkes, W. and Trowsdale, J. An ovarian tumor marker with homology to vaccinia virus contains an IgV-like region and multiple transmembrane domains. *Cancer Res.*, **52**, 5416–5420 (1992).
14) Brown, E. J. Signal transduction from leukocyte integrins. *In* "Cell Adhesion Molecules," ed. M. E. Hemler and E. Mihich, pp. 105–125 (1993). Plenum Press, New York.
15) Lindberg, F. P., Gresham, H. D., Schwarz, E. and Brown, E. Molecular cloning of integrin-associated protein: an immunoglobulin family member with multiple membrane-spanning implicated in $\alpha_v\beta_3$-dependent ligand binding. *J. Cell Biol.*, **123**, 485–496 (1993).
16) Schwartz, M. A., Brown, E. J. and Fazeli, B. A. 50-kDa integrin-associated protein is required for integrin-regulated calcium entry in endothelial cells. *J. Biol. Chem.*, **268**, 19931–19934 (1993).
17) Mawby, W. J., Holmes, C. H., Anstee, D. J., Spring, F. A. and Tanner, M. J. Isolation and characterization of CD47 glycoprotein: a multispanning membrane protein which is the same as integrin-associated protein (IAP) and the ovarian tumor marker OA3. *Biochem. J.*, **304:** 525–530 (1994).
18) Anstee, D. J. and Spring, F. A. White cell differentiation antigens. *In* "Leukocyte Typing V," ed. S. F. Schlossman, L. Boumsell, W. Gilks, J. M. Harlan, T. Kishimoto, C. Morimoto, J. Ritz, S. Shaw, R. Silverstein, T. Springer, T. F. Tedder and R. F. Todd, pp. 233–234 (1994). Oxford University Press, New York.
19) Hadam, M. R. White cell differentiation antigens. *In* "Leukocyte Typing IV," ed. W. Knapp, B. Dorken, W. R. Gilks, E. P. Rieber, R. E. Schmit, H. Stein and A. E. G. Kr. von dem Borne, pp. 658–661 (1989). Oxford University Press, New York.
20) Lindberg, F. P., Lublin, D. M., Telen, M. J., Veile, R. A., Miller, Y. E., Donis-Keller, H. and Brown, E. J. Rh-related antigen CD47 is the signal-transducer integrin-associated protein. *J. Biol. Chem.*, **269**, 1567–1570 (1994).
21) Mochizuki, T., Wu, G., Hayashi, T., Xenophontos, S. L., Veldhuisen, B., Saris, J. J., Reynolds, D. M., Cai, Y., Gabow, P. A., Pierides, A., Kimberling, W. J., Breuning, M. H., Deltas, C. C., Peters, D. J. M. and Somlo, S. PKD 2, a gene for polycystic kidney disease that encodes an integral membrane protein. *Science*, **272**, 1339–1342 (1996).
22) Dunnill, M. S., Millard, P. R. and Oliver, D. Acquired cystic disease of the kidneys: a hazard of long-term intermittent maintenance haemodialysis. *J. Clin. Pathol.*, **30**, 868–877 (1977).
23) Hughson, M. D., Buchwald, D. and Fox, M. Renal neoplasia and acquired cystic disease in patients receiving long-term dialysis. *Arch. Pathol. Lab. Med.*, **110**, 592–601 (1986).
24) Heino, J. Biology of tumor cell invasion: interplay of cell adhesion and matrix degradation. *Int. J. Cancer*, **65**, 717–722 (1996).
25) Liang, P. and Pardee, A. B. Differential display of eukaryotic messenger RNA by means of polymerase chain reaction. *Science*, **257**, 967–971 (1992).
26) Jung, M., Kondratyev, A. D. and Dritschilo, A. Elongation factor 1δ is enhanced following exposure to ionizing radiation. *Cancer Res.*, **54**, 2541–2543 (1994).
27) Watson, M. A. and Fleming, T. P. Isolation of differentially expressed sequence tags from human cancer. *Cancer Res.*, **54**, 4598–4602 (1994).
28) Crawford, D., Zbinden, I., Amstad, P. and Cerutti, P. Oxidant stress induces the proto-oncogenes c-*fos* and c-*myc* in mouse epidermal cells. *Oncogene*, **3**, 27–32 (1988).
29) Nose, K., Shibanuma, M., Kikuchi, K., Kageyama, H., Sakiyama, S. and Kuroki, T. Transcriptional activation of early-response genes by hydrogen peroxide in a mouse osteoblastic cell line. *Eur. J. Biochem.*, **201**, 99–106 (1991).
30) Mostofi, F. K. Histological typing of kidney tumors. *In* "International Histological Classification of Tumors, No. 25," ed. F. K. Mostofi (1981). WHO, Geneva.